separations

MDPI

Article

Green Preparation of ZnO Nanoparticles Using *Citrus aurantium* L. Extract for Dye Adsorption, Antibacterial, and Antioxidant Activities

Xitao Yang, Liangliang Liu, Chenxiao Chen, Liping Liao and Siqi Huang *

Institute of Bast Fiber Crops, Chinese Academy of Agricultural Sciences, Changsha 410205, China; 82101225155@caas.cn (X.Y.); liuliangliang@caas.cn (L.L.)
* Correspondence: huangsiqi@caas.cn; Tel.: +86-731-88998505

Abstract: In this study, ZnO nanoparticles (ZnO NPs) were synthesized using a green method employing fresh *Citrus aurantium* L. aqueous extract (CA) as a reducing agent. After preparation, the ZnO NPs were characterized by transmission electron microscopy (TEM), scanning electron microscopy (SEM), energy-dispersive X-ray analysis (EDAX), X-ray diffraction (XRD), and infrared spectroscopy (IR). The products displayed irregular particle shapes on a nanoscale. The adsorption ability of ZnO NPs was tested with amaranth red dye, and the result showed that it had a satisfied capacity for amaranth red. The adsorption data followed the pseudo-second-order model and the Langmuir model, which indicated the adsorption process was controlled by a chemical adsorption process and occurred homogeneously on the surface of absorbents. In addition, the prepared ZnO NPs also exhibited antibacterial abilities against *Staphylococcus aureus* and *Escherichia coli* bacteria; antioxidant activities were observed in 2-2-diphenyl-1-picrylhydrazyl (DPPH) and 2,2′-azino-di(3-ethylbenzthiazoline sulphonate) (ABTS) radicals scavenging assays and the ferric ion reducing antioxidant power (FRAP) assay, which were better than those of traditional ZnO NPs except in the FRAP assay. Based on these findings, the ZnO NPs fabricated with CA aqueous extract displayed promising abilities in the environmental remediation of dye wastewater.

Keywords: adsorption; amaranth red; antibacterial; antioxidant; *Citrus aurantium* L.

check for updates

Academic Editors: Gavino Sanna and Dimosthenis Giokas

Received: 12 October 2024
Revised: 17 January 2025
Accepted: 17 January 2025
Published: 21 January 2025

Citation: Yang, X.; Liu, L.; Chen, C.; Liao, L.; Huang, S. Green Preparation of ZnO Nanoparticles Using *Citrus aurantium* L. Extract for Dye Adsorption, Antibacterial, and Antioxidant Activities. *Separations* **2025**, *12*, 18. https://doi.org/10.3390/separations12020018

Copyright: © 2025 by the authors. Licensee MDPI, Basel, Switzerland. This article is an open access article distributed under the terms and conditions of the Creative Commons Attribution (CC BY) license (https://creativecommons.org/licenses/by/4.0/).

1. Introduction

With the progress and deepening of textile printing and dyeing processes, synthetic dyes have been widely used in various industries in recent decades. Therefore, a large amount of printing and dyeing wastewater is continuously discharged into the water environment through multiple channels, forming an important part of industrial wastewater discharge [1]. Due to the characteristics of this dyeing wastewater, like strong color, high toxicity levels, elevated concentrations of organic pollutants, and poor biodegradability, it contributes a serious threat to natural water quality [2]. In order to solve the problem of treating dye wastewater, a variety of scientific methods have been introduced, including the biological method, the photocatalytic method, and the physical method [3–6]. Among them, the physical method, especially the adsorption method, has attracted more and more attention due to its advantages: simple operation, high efficiency, absence of secondary pollution, economy, and practicality [7]. In this method, the adsorbent is the core factor affecting the efficiency and cost of the adsorption method in removing pollutants [8]. At present, most of the adsorbents have problems such as low adsorption capacity and difficulty in

regeneration during recycle usage, which limit the application of the adsorption method in wastewater treatment [9,10]. However, nanomaterials have shown great potential applications in many fields, such as biomedicine, environmental science, energy production, and other industries, because of their excellent physical and chemical properties and high biocompatibility [11]. The addition of nanomaterials is expected to improve the existing problems in adsorption research.

Zinc oxide nanoparticles (ZnO NPs) are a kind of inorganic nanomaterial. Their unique properties, including photocatalysis, antioxidant, antibacterial, and antifungal activities, make them highly valuable in many research fields [12]. The traditional synthesis methods of ZnO NPs are the hydrothermal method, the sol-gel method, the chemical precipitation method, and so on [13,14]. In recent years, the green synthesis technique has emerged as a promising approach to producing ZnO NPs that minimize the drawbacks [15]. The advantages of green synthesis approaches include a low rate of hazards, biocompatibility, eco-friendliness, effective scalability, and high cost-effectiveness [16]. Such processes utilize various low-cost and environmentally friendly materials, including plant-derived extracts, to facilitate the synthesis of ZnO NPs [17,18]. These plant-derived extracts are commonly rich in phytochemicals, such as tannins, amino acids, polyphenols, flavonoids, and alkaloids, which play crucial roles in preparing ZnO NPs due to their cost-effectiveness and reduced reliance on toxic chemicals. Many plant extracts have been reported in the green synthesis of ZnO NPs [19]. As per our previous report, the aqueous extract of *Hibiscus cannabinus* leaves was used as an additive in the synthesizing of ZnO NPs [20]. The products showed good adsorption capacity for dyes, as well as antioxidant and antibacterial activities.

Citrus aurantium L. (CA) is a member of the Rutaceae family and has a long history of cultivation in China. The fruit of CA (called Suancheng in Chinese) is not edible, and CA has been utilized as a medicinal plant in China [21]. For traditional Chinese medicinal usage, CA is primarily cultivated in Sichuan, Hunan, Jiangxi, and Zhejiang provinces, and has gradually developed as an iconic local product. CA has a wide range of pharmacological effects in treating various diseases [22]. It can play a role in regulating the gastrointestinal tract, and has anti-inflammatory, hepatoprotective, and antioxidant effects through different pathways and targets [23]. The main components in CA are flavonoids and alkaloids [24]. Flavonoids in CA mainly contain dihydroflavonoids and flavonoids, including hesperidin, naringin, neohesperidin, eriocitrin, neoeriocitrin, narirutin, hesperetin, naringenin, and neoeriocitrin [25]. The alkaloids in CA are reported to be synephrine, N-methyltyramine, quinoline, and so on [26].

The main purpose of this study was to achieve the green preparation of ZnO NPs in the presence of CA water extract, which served as a reducing agent. For better comparison, *Brassica rapa* L. var. *Chinensis* (BLC) extract was also obtained and used in the preparation of ZnO NPs. Moreover, the adsorption capacity of dyes, antioxidant activity, and antibacterial activity against *Staphylococcus aureus* (*S. aureus*) and *Escherichia coli* (*E. coli*) of synthesized ZnO NPs were studied. Analyses of the morphology, size, elemental composition, and structure of the synthesized ZnO NPs were conducted; the results were compared with those of normal ZnO NPs without natural extracts through transmission electron microscopy (TEM), scanning electron microscopy (SEM), energy-dispersive X-ray analysis (EDAX), X-ray diffraction (XRD), and infrared spectroscopy (IR). Amaranth red was used as the adsorption target compound for the adsorption study. To better show the advantages of green-prepared ZnO NPs, the antioxidant abilities were evaluated by the 2-2-diphenyl-1-picrylhydrazyl (DPPH), 2,2′-azino-di(3-ethylbenzthiazoline sulpho-nate) (ABTS), and ferric reducing antioxidant power (FRAP) radical scavenging tests.

2. Materials and Methods

2.1. Materials

In this study, the reagents were bought from Macklin Inc. (Shanghai, China) in analytical grade and directly used. *Citrus aurantium* L. (CA) was planted in the experimental base of the Institute of Bast Fiber Crops, Chinese Academy of Agricultural Sciences in 2023 and 2024. The harvest time of CA sample is 60 days after flowering. The *Brassica rapa* L. var. *Chinensis* (BLC) samples were bought from the local market and washed with water for further use. The collected fresh CA fruits and BLC were dried to constant weight in an oven at 55 °C, grounded into powders, and stored in sealed bags at 4 °C.

2.2. Extraction of CA and BLC

Measurements of 20 g of CA or BLC powders were rinsed in 200 mL of ethanol solution (10%). Under magnetic stirring, the mixture was extracted at 90 °C for 2 h. After cooling, the solvents were filtrated by filter and stored at 4 °C for further use. The products were marked as CA extract and BLC extract.

2.3. Preparation of ZnO NPs, ZnO NPs-B, and ZnO NPs-CK

The sodium hydroxide solution (0.2 mol/L) was dropped into the zinc sulfate solution (0.02 mol/L) containing 10 mL of CA extract. With the addition of an alkaline solution, the pH of the mixture was changed to 8.5, and the mixture was incubated at 40 °C under magnetic stirring for 3 h. Finally, the solid product was centrifuged and washed with water. After drying at 80 °C in the oven, the product was ground into powders for storage and use. When the same amount of BLC extract was used instead of the CA extract, the product was marked as ZnO NPs-B. Meanwhile, the same amount of water was used instead of the CA extract, and the product was marked as ZnO NPs-CK.

The prepared products were characterized by SEM (Apreo 2 Thermo Scientific, Waltham, MA, USA) equipped with an X-ray fluorescence spectrometer Oxford INCA X-max 80 for EDAX, TEM (JEOL JEM-F200, Tokyo, Japan) operating at 200 kV, XRD (Rigaku SmartLab 9, Tokyo, Japan) using Cu-Kα radiation at 40 kV and 40 mA, and IR analysis (Shimadzu IR Spirit spectrophotometer, Tokyo, Japan).

2.4. Adsorption Assay

Certain amounts of prepared ZnO NPs were dispersed in 50 mL of the aqueous amaranth red with different concentrations. The mixture was shaken on an oscillator for adsorption experiments. When the experimental times reached, 0.5 mL of the mixture was obtained, filtrated by a 0.45 μm filter, and detected on a UV2700 UV-Vis spectrophotometer (Shimadzu, Kyoto, Japan) at 510 nm. The adsorption rate was calculated by Equation (1):

$$q_t = \frac{(C_i - C_t) \times V}{w} \quad (1)$$

where q_t is the adsorbed amount of amaranth red on the ZnO NPs at a certain time, C_i is the initial concentration of amaranth red, C_t is the concentration of amaranth red at a certain time, V is the volume of solution for adsorption, and w is the weight of absorbents used [27].

For adsorption kinetics assays, 0.3 g of ZnO NPs were dispersed in 50 mL of the aqueous amaranth red at 1.0 g/L. At certain time intervals, 0.5 mL of mixture was obtained, filtrated, and detected. The data were fitted to the pseudo-first-order and pseudo-second-order kinetic models. The pseudo-first-order and pseudo-second-order models are expressed using Equations (2) and (3), as follows:

$$\log(q_e - q_t) = \log q_e - K_1 t \quad (2)$$

$$\frac{t}{q_t} = \frac{1}{K_2 q_e^2} + \frac{t}{q_e} \quad (3)$$

where q_t is the adsorption rate, q_e is the adsorption rate in equilibrium, and K_1 and K_2 are, respectively, the rate constants of the two models [28].

For the adsorption isotherm assays, 0.3 g of ZnO NPs was dispersed in 50 mL of the aqueous amaranth red at different concentrations from 1.0 g/L to 5.0 g/L. After the equilibrium, 0.5 mL of the mixture was obtained, filtrated, and detected. The data were fitted to the Langmuir and Freundlich isotherms. The equations for the Langmuir and Freundlich isotherms can be expressed using Equations (4) and (5), as follows:

$$\frac{C_e}{q_e} = \frac{C_e}{q_m} + \frac{1}{K_l q_m} \quad (4)$$

$$\log q_e = \log K_f + \frac{1}{n} \log C_e \quad (5)$$

where C_e is the concentration of amaranth red in equilibrium, q_m is the maximum adsorption rate, $1/n$ is the adsorption intensity, and K_l and K_f are, respectively, the coefficients [29].

2.5. Antibacterial Activity

The antibacterial activity of the ZnO NPs was tested by Shanmugam's method with some modifications [30]. *S. aureus* and *E. coli* bacteria were used in this test. Measures of 0.05 mg, 0.1 mg, 0.2 mg, 0.3 mg, 0.5 mg, and 1.0 mg of the ZnO NPs were put in the wells of a sterile 96-well plate containing 180 µL of the nutrient broth. Then, 20 µL of the bacterial solution (1×10^{-6} CFU) was added in each well and the plate was incubated at 37 °C. The absorbance of each well was measured by an Epoch microplate reader (BioTek Instruments Inc., Winooski, VT, USA) at 600 nm. The nutrient broth without the addition of samples was used as a control.

2.6. Antioxidant Activity

2.6.1. DPPH Assay

The antioxidant activities of the ZnO NPs, ZnO NPs-B, and ZnO NPs-CK were tested by DPPH assay according to a previous report [20].

2.6.2. ABTS Assay

The antioxidant activities of the ZnO NPs, ZnO NPs-B, and ZnO NPs-CK were tested by ABTS assay according to a previous report [20].

2.6.3. FRAP Assay

FRAP was determined using a Solaibao BC1310 Total Antioxidant Capacity (T-AOC) detection kit. Reagent 1, Reagent 2, and Reagent 3 were mixed in a ratio of 7:1:1 to prepare a working solution. The standard curve at 593 nm was measured and drawn using a series of $FeSO_4$ standard solutions reacting with the FRAP working solution [31]. Several amounts of ZnO NPs (ZnO NPs-B and ZnO NPs-CK) were added into 500 µL of the FRAP working solution and reacted at room temperature for 10 min. After that, the absorbance at 593 nm was measured.

3. Results and Discussion

3.1. Characterizations of ZnO NPs

3.1.1. SEM with EDAX

SEM was employed for the morphological characterization of ZnO NPs (Figure 1a). As can be seen in the image, the small particles were aggregated to form a larger particle.

The shape of the ZnO NPs appeared as irregular particles, and the size was in the nanoscale. The elemental compositions of the ZnO NPs and ZnO NPs prepared without extract (ZnO NPs-CK) were analyzed and compared using EDAX in conjunction with SEM (Table 1). Three elements were calculated, including N, O, and Zn. Ultimately, the composition of oxygen in the ZnO NPs was increased by approximately 15 percent compared to ZnO NPs-CK. The higher content of oxygen and the presence of nitrogen may be attributed to the introduction of natural compounds from the extract.

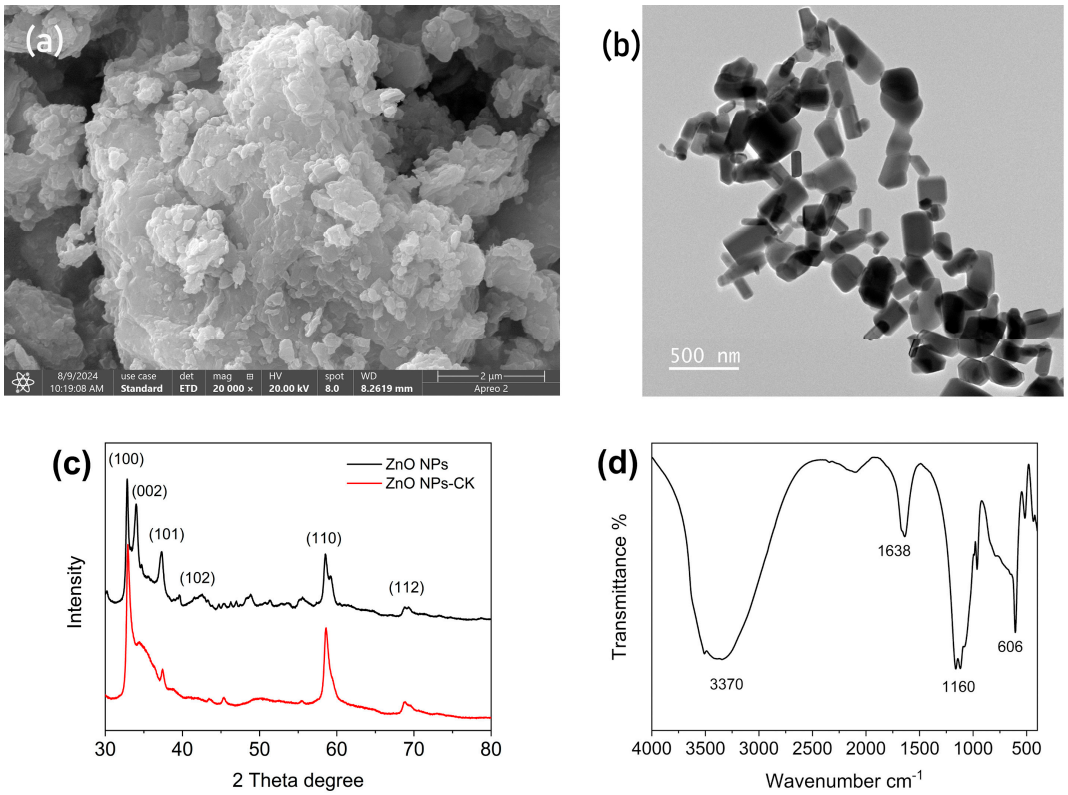


Figure 1. (**a**) SEM image of the ZnO NPs; (**b**) TEM image of the ZnO NPs; (**c**) XRD patterns of ZnO NPs (black line) and ZnO NPs-CK (red line) (the range of 2θ was from 30° to 80°); (**d**) IR spectrum of the ZnO NPs.

Table 1. The atom percentages of Zn NPs and Zn NPs-CK by EDAX.

Element	Zn NPs (At%)	Zn NPs-CK (At%)
N	0.25	0
O	75.54	60.43
Zn	24.21	39.57

3.1.2. TEM

TEM was also used to analyze the size and morphology of the prepared ZnO NPs, which was shown in Figure 1b. The shape and size of the ZnO NPs could be observed more clearly in TEM, which showed both block and sphere shapes with nonuniform sizes. The size distribution of the products was from 100 nm to 300 nm. However, the products were still functional for further usage.

3.1.3. XRD

According to the reference, the XRD patterns of the prepared ZnO NPs and ZnO NPs-CK were characterized from 30° to 80° of 2θ (Figure 1c) [32]. As the presented result, the XRD pattern exhibited peaks at 32.9°, 34.1°, 37.4°, 47.5°, 58.6°, and 69.34°, which could

be assigned to the planes (100), (002), (101), (102), (110), and (112), respectively [33]. This confirmed the formation of ZnO NPs. However, there are numerous peaks surrounding the mentioned peaks, and the 47.5° and 69.34° were not particularly apparent. The XRD pattern of ZnO NPs-CK exhibited similar peaks as well, and some peaks were not as apparent as those in the ZnO NPs. The addition of CA extract did not weaken the crystallization of the ZnO NPs.

3.1.4. IR

The IR spectrum of the ZnO NPs was shown in Figure 1d. In the range of 400–4000 cm^{-1}, the broad peak at 3370 cm^{-1} could be assigned as the primary amine and amide (O-H stretching) groups [34]. The peak at 1638 cm^{-1} was because of the stretching bend of the C-H bond of alkane [35]. The peaks around 1160 cm^{-1} were due to the C-O ether bond of the glucose ring of starch [36]. Another absorption peak could be observed around 606 cm^{-1}, which corresponded to the Zn-O vibration [37]. In summary, these IR peaks showed that the prepared ZnO NPs had typical groups.

3.2. Adsorption of Amaranth Red

3.2.1. The Adsorption Abilities of ZnO NPs

The adsorption rates of amaranth red using ZnO NPs, ZnO NPs-B, and ZnO NPs-CK were compared. As a result in Figure 2a, three kinds of ZnO NPs showed similar adsorption ability. Only a little advantage of ZnO NPs could be observed.

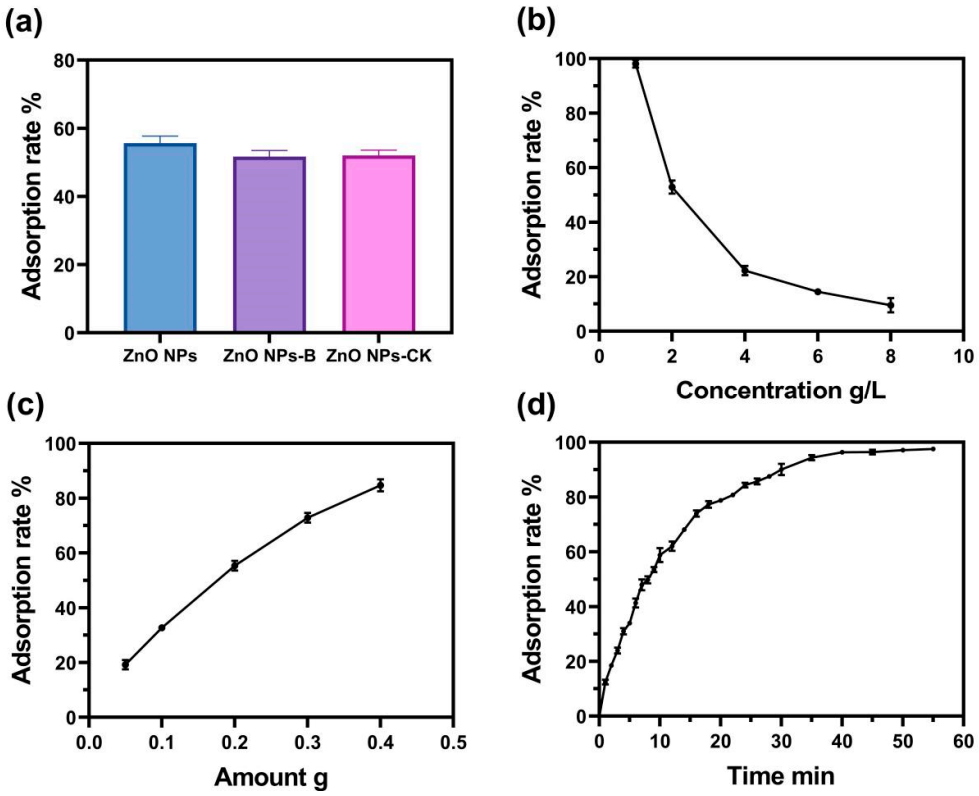


Figure 2. (**a**) Comparison of the adsorption rate among ZnO NPs, ZnO NPs-B, and ZnO NPs-CK (the concentration of amaranth red was 2 g/L, the amount of used absorbents was 0.2 g, the adsorption time was 2 h); (**b**) effect of the initial concentration of amaranth red on the adsorption rate (the amount of used absorbents was 0.2 g, the adsorption time was 2 h); (**c**) effect of the adsorbent amount on the adsorption rate (the concentration of amaranth red was 2 g/L, the adsorption time was 2 h); (**d**) effect of the adsorption time on the adsorption rate (the amount of used absorbents was 0.2 g, and the concentration of amaranth red was 1 g/L).

3.2.2. Effect of the Initial Concentration of Amaranth Red

The adsorption rates of amaranth red at different concentrations were studied using prepared ZnO NPs. As a result, as shown in Figure 2b, with the concentrations of amaranth red increased, the adsorption rates dropped accordingly. This kind of trend has often been observed in the related research. The usual explanation for this is that, since the amount of absorbents was certain, the adsorption sites were limited. With the increasing concentrations of amaranth red, the target molecules were increased. The sites were all occupied, resulting in a decrease in adsorption rates [38].

3.2.3. Effect of Adsorbent Amount

The adsorption rates of amaranth red at different amounts of adsorbents were studied. The use of ZnO NPs varied from 0.05 g to 0.4 g. According to the result shown in Figure 2c, when the amount of adsorbent increased, the adsorption rates increased as well. The highest adsorption rate was reached when the usage of adsorbent was highest. It could be assumed that, when the adsorbent usage increased, more sites for amaranth red were available, which have been reported by other references [39].

3.2.4. Effect of Adsorption Time

The adsorption rates of amaranth red at different adsorption times from 0 min to 60 min were studied. According to the result shown in Figure 2d, the adsorption rates increased gradually as the adsorption time went on, and finally reached saturation when the time was more than 40 min. This result suggested that the adsorption needed a certain time. When the time was more than 40 min, the active sites were almost saturated, leading to a steady adsorption rate [38]. Hence, the adsorption time was set at 40 min.

3.3. Adsorption Kinetics Study

In order to investigate the adsorption kinetics of amaranth red by using ZnO NPs, the pseudo-first-order model and the pseudo-second-order model were calculated [40]. According to the result shown in Figure 3, the data were generally fitted with these two models. The correlation coefficient of the model is closer to 1, indicating that the model is more suitable in explaining the mechanism of adsorption [40]. The correlation coefficients of the pseudo-first-order and pseudo-second-order models were calculated as 0.9796 and 0.9967, respectively. Based on these data, it could be found that the pseudo-second-order model had a higher fitting result and was more suitable for explaining the molecular interaction between the dyes and the adsorbents. The pseudo-second-order model assumed that the interaction of amaranth red and ZnO NPs was mainly controlled by a chemical adsorption process [41].

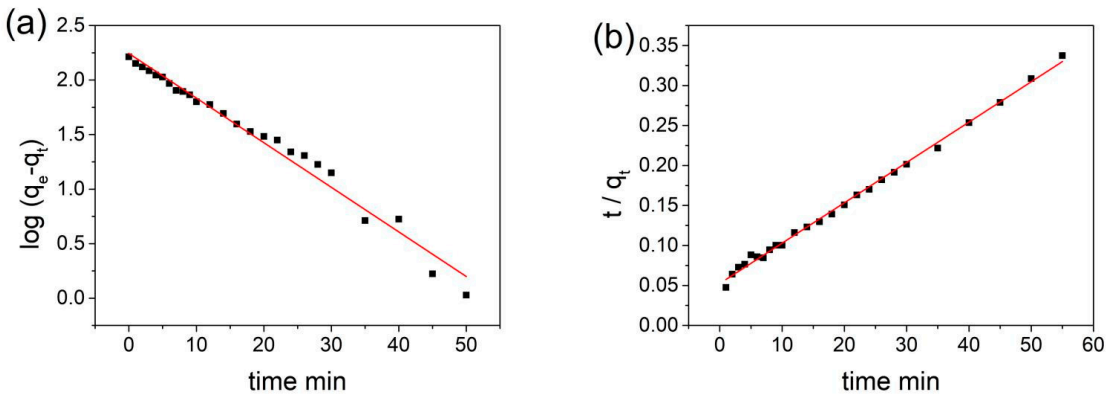


Figure 3. The linear fitting of kinetic models for the adsorption: (**a**) pseudo-first order and (**b**) pseudo-second order (the black dots are the experimental data, and the red lines are the fitting results).

3.4. Adsorption Isotherm Study

For investigating the adsorption isotherm of amaranth red by using ZnO NPs, the Langmuir isotherm and Freundlich isotherm models were used [42]. According to the results shown in Figure 4, the calculated data were fitted with two models, and the correlation coefficients of the Langmuir and Freundlich isotherm models were 0.9948 and 0.3160, respectively. Apparently, the correlation coefficient of the Langmuir model was much higher. Even when the most deviated data were deleted, the correlation coefficient of the Freundlich model was lower than 0.99. The better fitness for the Langmuir model indicates that homogeneous adsorption happened on the surface of ZnO NPs for amaranth red molecules [43].

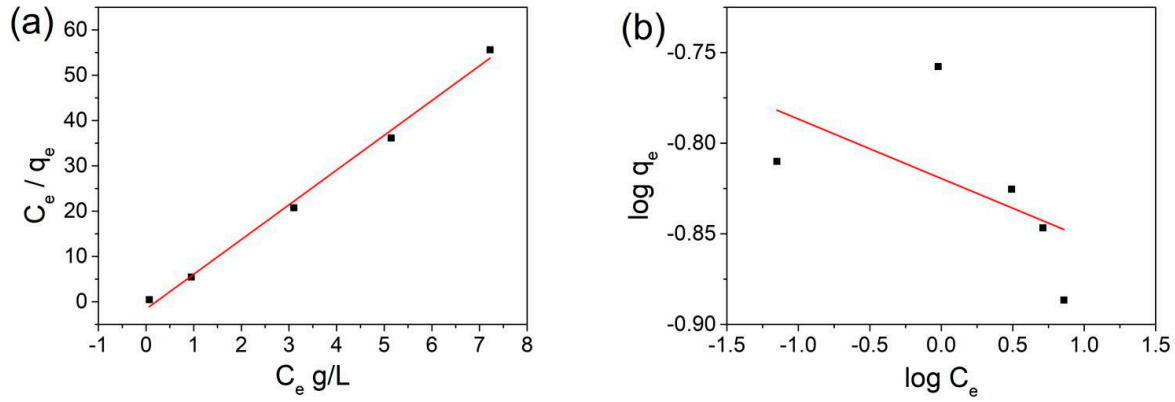


Figure 4. The linear fitting of isotherm models for the adsorption: (**a**) Langmuir isotherm and (**b**) Freundlich isotherm (the black dots are the experimental data, and the red lines are the fitting results).

3.5. Antibacterial Activity of ZnO NPs

As shown in Figure 5, when the concentrations of ZnO NPs were changed from 0.25 mg/mL to 5.0 mg/mL, the growth of bacteria was slowed down apparently, which indicated the positive antibacterial activity of prepared ZnO NPs. When the green synthesized ZnO NPs were about 0.25 mg/mL, the growth of *S. aureus* and *E. coli* were, respectively, stopped. The results demonstrated that the ZnO NPs could affect the growth of *S. aureus* and *E. coli* and could inhibit growth at certain concentrations. Cheperli's group reported the bacteriostatic and bactericidal effects of ZnO NPs prepared with extracts of *Malva neglecta* Wallr [44]. The materials had MIC values of 31.25 µg/L and 62.5 µg/L, respectively, against *E. coli* and *S. aureus*. They assumed that ZnO inhibits bacterial growth by causing damage to the cell membrane or extrusion of cytoplasmic content. Aya Elbrolesy prepared ZnO NPs using *Solanum Lycopersicum* extract [45]. The synthesized ZnO NPs showed significant antibacterial activity on *S. aureus* and *E. coli*. They thought the possible mechanism relies on electrostatic forces, mechanical destruction of the bacterial cell membrane, and the release of Zn^{2+} ions [46,47].

3.6. Antioxidant Activities of ZnO NPs

Oxidative stress is a negative effect produced by free radicals in the body and is considered to be an important factor in aging and disease. Oxidative stress refers to the imbalance between oxidation and antioxidants in the body, which tends to oxidize, resulting in inflammatory infiltration of neutrophils, increased protease secretion, and the production of a large number of oxidative intermediates [48–50]. The ABTS assays and the DPPH assays are among the most abundant antioxidant capacity assays [51]. The FRAP method is an experimental method used to detect the total antioxidant capacity. By measuring the absorbance of the characteristic absorption peak at 593 nm, the antioxidant capacity

of the sample can be calculated. This method is not only simple and fast, it can also can reflect the reduction capacity of the sample to be tested to a certain extent; that is, it can be used to determine the total antioxidant capacity of the sample [52,53]. The above three methods were used to determine the antioxidant properties of ZnO NPs, ZnO NPs-B, and ZnO NPs-CK. Figure 6 shows the antioxidant activities of ZnO NPs, ZnO NPs-B, and ZnO NPs-CK on DPPH, ABTS, and FRAP assays. The scavenging activities of ZnO NPs at different concentrations were 4.76% to 22.75% for DPPH, 84.61% to 91.70% for ABTS, and 9.82% to 30.94% for FRAP. In contrast, the scavenging activities of ZnO NPs prepared without extract (ZnO NPs-CK) at different concentrations were 3.15% to 12.31% for DPPH, 45.79% to 51.78% for ABTS, and 17.03% to 43.26% for FRAP. It could be found from the results that the scavenging activities of ABTS and DPPH by ZnO NPs were higher than those of ZnO NPs-CK, indicating that the extracts contributed to the antioxidant capacity. However, for FRAP, the antioxidant activity of ZnO NPs-CK was better than that of ZnO NPs. As a comparison group, the scavenging activities of ZnO NPs-B were similar to those of ZnO NPs-CK. The changes were not apparent. The results showed that the addition of CA extract in the preparation of ZnO NPs contributed to a good improvement in the scavenging activities for DPPH and ABTS. Meanwhile, the usage of BLC extract could not achieve this effect. As reported by Donmez [54] and Tiwari [55], ZnO NPs synthesized from different plant materials and their antioxidant properties were measured. Good scavenging abilities for DPPH and ABTS were exhibited by the ZnO NPs synthesized from plant materials; this finding is consistent with those of this study.

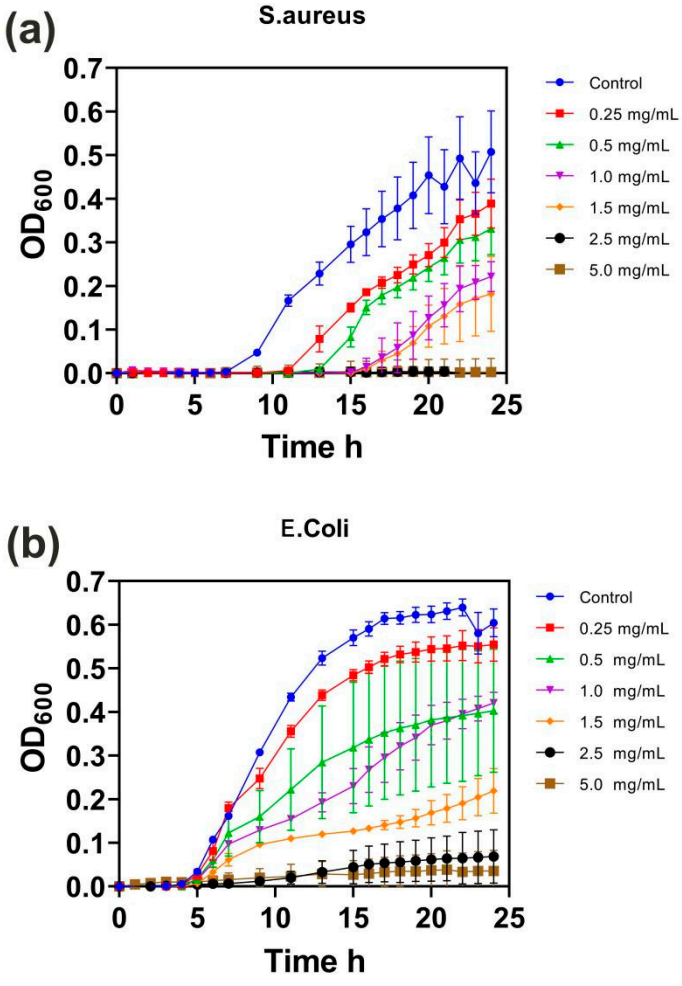


Figure 5. The growth curves of (**a**) *S. aureus* and (**b**) *E. coli* with different concentrations of ZnO NPs.

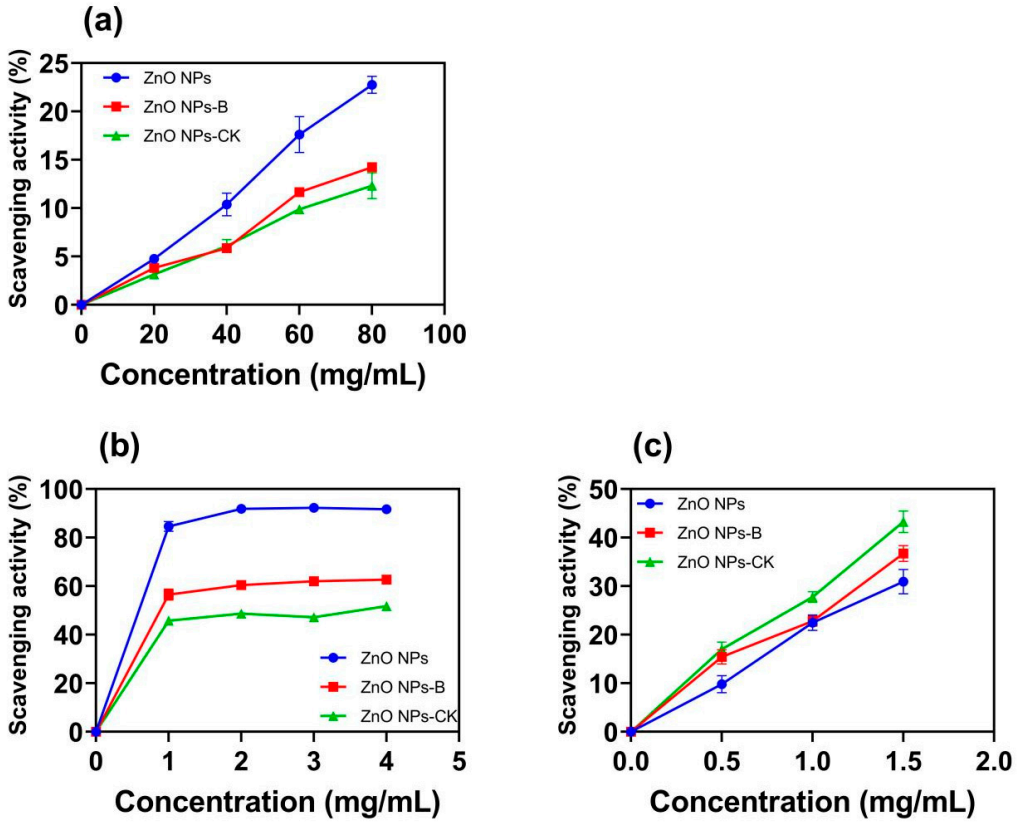


Figure 6. The scavenging activities of ZnO NPs, ZnO NPs-B, and ZnO NPs-CK for (**a**) DPPH free radicals, (**b**) ABTS free radicals, and (**c**) FRAP assays.

4. Conclusions

The green synthesis method, used to produce ZnO NPs using CA aqueous extract, was well characterized using TEM, SEM, EDAX, IR, and XRD. The products showed typical characteristics of ZnO NPs and some organic compounds on the surface. The prepared ZnO NPs demonstrated good adsorption efficiency for amaranth red. The influencing factors during adsorption were determined, and the results showed the adsorption process followed the pseudo-second-order kinetic and the Langmuir isotherm. These results indicated that the adsorption process was controlled by a chemical adsorption process and occurred homogeneously on the surface of the absorbents. In the antibacterial assay, the ZnO NPs displayed strong antibacterial activities against *S. aureus* and *E. coli*. The presence of ZnO NPs at 0.25 mg/mL could stop the growth of *S. aureus* and *E. coli*, respectively. In antioxidant assays, three kinds of tests showed the apparent radical scavenging ability of ZnO NPs. Except for FRAP, the scavenging activities of ABTS and DPPH by ZnO NPs were higher than those of ZnO NPs-B and ZnO NPs-CK. This environmentally friendly synthesis method produced ZnO NPs with excellent adsorption capabilities, antioxidant and antibacterial activities, and significant potential for environmental remediation applications.

Author Contributions: Conceptualization, L.L. (Liangliang Liu); Data curation, X.Y.; Formal analysis, C.C.; Methodology, L.L. (Liping Liao); Project administration, S.H.; Writing—original draft, L.L. (Liangliang Liu) and S.H.; Writing—review and editing, S.H. All authors have read and agreed to the published version of the manuscript.

Funding: This work was supported by the Science and Technology Innovation Program of Hunan Province (No. 2022RC3059), the Agriculture Research System of China (CARS-19-E22), the Chinese Agricultural Science and Technology Innovation Project (ASTIP-IBFC-05), the Central Public-interest Scientific Institution Basal Research Fund (No. 1610242024010, No. 1610242024006, No. Y2023XK14).

Data Availability Statement: The data presented in this study are available on request from the corresponding authors. The data are not publicly available due to security requirements in the institute of the corresponding author.

Conflicts of Interest: The authors declare no conflicts of interest.

References

1. Song, Y.; Wang, L.; Qiang, X.; Gu, W.; Ma, Z.; Wang, G. An Overview of Biological Mechanisms and Strategies for Treating Wastewater from Printing and Dyeing Processes. *J. Water Process Eng.* **2023**, *55*, 104242. [CrossRef]
2. Ceylan, E.; Dindaş, G.B.; Bektaş, N.; Yatmaz, H.C. Modification of Natural Chitosan with Fe and Ce Cations as Photocatalyst Beads: Degradation of Dye Chemicals and Textile Wastewater under UVA Light. *J. Environ. Manag.* **2022**, *310*, 114790. [CrossRef] [PubMed]
3. Tianzhi, W.; Weijie, W.; Hongying, H.; Khu, S.-T. Effect of Coagulation on Bio-Treatment of Textile Wastewater: Quantitative Evaluation and Application. *J. Clean. Prod.* **2021**, *312*, 127798. [CrossRef]
4. Thanh Tu, N.T.; Thien, T.V.; Du, P.D.; Thanh Chau, V.T.; Mau, T.X.; Khieu, D.Q. Adsorptive Removal of Congo Red from Aqueous Solution Using Zeolitic Imidazolate Framework–67. *J. Environ. Chem. Eng.* **2018**, *6*, 2269–2280. [CrossRef]
5. Qin, L.; Gao, M.; Zhang, M.; Feng, L.; Liu, Q.; Zhang, G. Application of Encapsulated Algae into MBR for High-Ammonia Nitrogen Wastewater Treatment and Biofouling Control. *Water Res.* **2020**, *187*, 116430. [CrossRef] [PubMed]
6. Samsami, S.; Mohamadizaniani, M.; Sarrafzadeh, M.-H.; Rene, E.R.; Firoozbahr, M. Recent Advances in the Treatment of Dye-Containing Wastewater from Textile Industries: Overview and Perspectives. *Process Saf. Environ. Prot.* **2020**, *143*, 138–163. [CrossRef]
7. Laskar, N.; Kumar, U. Application of Low-Cost, Eco-Friendly Adsorbents for the Removal of Dye Contaminants from Wastewater: Current Developments and Adsorption Technology. *Environ. Qual. Manag.* **2022**, *32*, 209–221. [CrossRef]
8. Teo, S.; Ng, C.; Islam, A.; Abdulkareem-Alsultan, G.; Joseph, C.; Janaun, J.; Taufiq-Yap, Y.; Khandaker, S.; Islam, G.; Znad, H.; et al. Sustainable Toxic Dyes Removal with Advanced Materials for Clean Water Production: A Comprehensive Review. *J. Clean. Prod.* **2022**, *332*, 130039. [CrossRef]
9. Rashid, R.; Shafiq, I.; Akhter, P.; Iqbal, M.; Hussain, M. A State-of-the-Art Review on Wastewater Treatment Techniques: The Effectiveness of Adsorption Method. *Environ. Sci. Pollut. Res.* **2021**, *28*, 9050–9066. [CrossRef] [PubMed]
10. Baskar, A.V.; Bolan, N.; Hoang, S.A.; Sooriyakumar, P.; Kumar, M.; Singh, L.; Jasemizad, T.; Padhye, L.P.; Singh, G.; Vinu, A.; et al. Recovery, Regeneration and Sustainable Management of Spent Adsorbents from Wastewater Treatment Streams: A Review. *Sci. Total Environ.* **2022**, *822*, 153555. [CrossRef] [PubMed]
11. Selmani, A.; Kovačević, D.; Bohinc, K. Nanoparticles: From Synthesis to Applications and Beyond. *Adv. Colloid Interface Sci.* **2022**, *303*, 102640. [CrossRef] [PubMed]
12. Zhou, X.-Q.; Hayat, Z.; Zhang, D.-D.; Li, M.-Y.; Hu, S.; Wu, Q.; Cao, Y.-F.; Yuan, Y. Zinc Oxide Nanoparticles: Synthesis, Characterization, Modification, and Applications in Food and Agriculture. *Processes* **2023**, *11*, 1193. [CrossRef]
13. Mishra, P.K.; Mishra, H.; Ekielski, A.; Talegaonkar, S.; Vaidya, B. Zinc Oxide Nanoparticles: A Promising Nanomaterial for Biomedical Applications. *Drug Discov. Today* **2017**, *22*, 1825–1834. [CrossRef]
14. Singh, T.A.; Das, J.; Sil, P.C. Zinc Oxide Nanoparticles: A Comprehensive Review on Its Synthesis, Anticancer and Drug Delivery Applications as Well as Health Risks. *Adv. Colloid Interface Sci.* **2020**, *286*, 102317. [CrossRef]
15. Nizamuddin, S.; Hymavathi, A.; Yaku, G.; Kumar, U. Green Synthesis and Characterization of ZnO Nanoparticles-A Novel Approach Using Carica Papaya Leaf Extract. *Mater. Today Proc.* **2022**, *62*, 6854–6856. [CrossRef]
16. López-Cuenca, S.; Salazar-Peña, R.; Pedroza-Toscano, M. Green Synthesis of Zinc Oxide Nanoparticles: Anticancer and Antibacterial Applications (A Review). *Russ. J. Gen. Chem.* **2024**, *94*, 2338–2355. [CrossRef]
17. Kazemi, S.; Hosseingholian, A.; Gohari, S.D.; Feirahi, F.; Moammeri, F.; Mesbahian, G.; Moghaddam, Z.S.; Ren, Q. Recent Advances in Green Synthesized Nanoparticles: From Production to Application. *Mater. Today Sustain.* **2023**, *24*, 100500. [CrossRef]
18. Haque, M.J.; Bellah, M.M.; Hassan, M.R.; Rahman, S. Synthesis of ZnO Nanoparticles by Two Different Methods & Comparison of Their Structural, Antibacterial, Photocatalytic and Optical Properties. *Nano Express* **2020**, *1*, 010007. [CrossRef]
19. Jadoun, S.; Arif, R.; Jangid, N.; Meena, R. Green Synthesis of Nanoparticles Using Plant Extracts: A Review. *Environ. Chem. Lett.* **2021**, *19*, 355–374. [CrossRef]
20. Yang, X.; Cao, X.; Chen, C.; Liao, L.; Yuan, S.; Huang, S. Green Synthesis of Zinc Oxide Nanoparticles Using Aqueous Extracts of *Hibiscus cannabinus* L.: Wastewater Purification and Antibacterial Activity. *Separations* **2023**, *10*, 466. [CrossRef]
21. Maksoud, S.; Abdel-Massih, R.M.; Rajha, H.N.; Louka, N.; Chemat, F.; Barba, F.J.; Debs, E. *Citrus aurantium* L. Active Constituents, Biological Effects and Extraction Methods. An Updated Review. *Molecules* **2021**, *26*, 5832. [CrossRef]
22. Ren, W.; Wang, S.; Zhang, J.; Liu, D. Ethnopharmacology, Chemical Composition and Functions of *Citrus aurantium* L. *J. Food Meas. Charact.* **2024**, *18*, 8843–8864. [CrossRef]

23. Zahr, S.; Zahr, R.; El Hajj, R.; Khalil, M. Phytochemistry and Biological Activities of *Citrus Sinensis* and *Citrus Limon*: An Update. *J. Herb. Med.* **2023**, *41*, 100737. [CrossRef]
24. Suntar, I.; Khan, H.; Patel, S.; Celano, R.; Rastrelli, L. An Overview on *Citrus aurantium* L.: Its Functions as Food Ingredient and Therapeutic Agent. *Oxid. Med. Cell. Longev.* **2018**, *2018*, 7864269. [CrossRef]
25. Koolaji, N.; Shammugasamy, B.; Schindeler, A.; Dong, Q.; Dehghani, F.; Valtchev, P. Citrus Peel Flavonoids as Potential Cancer Prevention Agents. *Curr. Dev. Nutr.* **2020**, *4*, nzaa025. [CrossRef]
26. Klimek-Szczykutowicz, M.; Szopa, A.; Ekiert, H. Citrus Limon (Lemon) Phenomenon—A Review of the Chemistry, Pharmacological Properties, Applications in the Modern Pharmaceutical, Food, and Cosmetics Industries, and Biotechnological Studies. *Plants* **2020**, *9*, 119. [CrossRef]
27. Jangra, A.; Singh, J.; Kumar, J.; Rani, K.; Kumar, P.; Kumar, S.; Singh, D.; Kumar, R. Dye Elimination by Surface-Functionalized Magnetite Nanoparticles: Kinetic and Isotherm Studies. *Biointerface Res. Appl. Chem.* **2022**, *13*, 325. [CrossRef]
28. Kandasamy, S.; Velusamy, S.; Thirumoorthy, P.; Periyasamy, M.; Veerasamy, S.; Gopalakrishnan, K.M.; Sathish, U.; Kiramani, V.; Antrini, F.D.G.; Periyasamy, S. Adsorption of Chromium Ions from Aqueous Solutions by Synthesized Nanoparticles. *J. Nanomater.* **2022**, *2022*, 6214438. [CrossRef]
29. Wang, T.; Zhong, X.; Zhang, Z.; Yuan, X.; Zhou, L.; Zheng, Z.; Farhadian, A.; Hu, J. Asphaltene Adsorption of Co_3O_4 Nanoparticles Modified by SiO_2 Film. *Appl. Surf. Sci.* **2022**, *602*, 154267. [CrossRef]
30. Agarwal, H.; Nakara, A.; Menon, S.; Shanmugam, V. Eco-Friendly Synthesis of Zinc Oxide Nanoparticles Using Cinnamomum Tamala Leaf Extract and Its Promising Effect towards the Antibacterial Activity. *J. Drug Deliv. Sci. Technol.* **2019**, *53*, 101212. [CrossRef]
31. Jiménez-Morales, W.A.; del P. Cañizares-Macias, M. Fast FRAP-SIA Method to Determine Antioxidant Capacity. *Talanta* **2024**, *273*, 125813. [CrossRef] [PubMed]
32. Kiran Kumar, A.B.V.; Saila, E.S.; Narang, P.; Aishwarya, M.; Raina, R.; Gautam, M.; Shankar, E.G. Biofunctionalization and Biological Synthesis of the ZnO Nanoparticles: The Effect of Raphanus Sativus (White Radish) Root Extract on Antimicrobial Activity against MDR Strain for Wound Healing Applications. *Inorg. Chem. Commun.* **2019**, *100*, 101–106. [CrossRef]
33. Khan, M.M.; Saadah, N.H.; Khan, M.E.; Harunsani, M.H.; Tan, A.L.; Cho, M.H. Potentials of Costus Woodsonii Leaf Extract in Producing Narrow Band Gap ZnO Nanoparticles. *Mater. Sci. Semicond. Process.* **2019**, *91*, 194–200. [CrossRef]
34. Alalawy, A.I.; Saleh, F.M.; Saeedi, N.H.; Panneerselvam, C.; Sakran, M.I.; Khasim, S.; Parveen, H.; Mohammedsaleh, Z.M.; Mukhtar, S.; Faridi, U.; et al. Green Synthesis of Bb-ZnO NPs Using Barleria Buxifolia Leaf Extract: Investigations into Their Physicochemical, Biological and Anti-Cancer Properties. *Polyhedron* **2025**, *267*, 117366. [CrossRef]
35. Yadav, A.; Kumar, H.; Kumar, P.; Rani, G.; Maken, S. Syzygium Cumini Leaf Extract Mediated Green Synthesis of ZnO Nanoparticles: A Sustained Release for Anticancer, Antimicrobial, Antioxidant, and Anti-Corrosive Applications. *J. Mol. Struct.* **2025**, *1325*, 141017. [CrossRef]
36. Sharma, A.; Nagraik, R.; Venkidasamy, B.; Khan, A.; Dulta, K.; Kumar Chauhan, P.; Kumar, D.; Shin, D.-S. In Vitro Antidiabetic, Antioxidant, Antimicrobial, and Cytotoxic Activity of Murraya Koenigii Leaf Extract Intercedes ZnO Nanoparticles. *Luminescence* **2023**, *38*, 1139–1148. [CrossRef] [PubMed]
37. Ramírez, J.I.; Villegas, V.A.; Sicairos, S.P.; Guevara, E.H.; Brito Perea, M.D.; Sánchez, B.L. Synthesis and Characterization of Zinc Peroxide Nanoparticles for the Photodegradation of Nitrobenzene Assisted by UV-Light. *Catalysts* **2020**, *10*, 1041. [CrossRef]
38. Açıkgöz, M.; Rahmanberdyyev, N.; Başkan, G. Olive Leaf Extract-Assisted Preparation of Nanoferrite for Adsorptive Removal of Cationic Dye. *Mater. Chem. Phys.* **2024**, *323*, 129662. [CrossRef]
39. Mozafarjalali, M.; Hamidian, A.H.; Sayadi, M.H. Microplastics as Carriers of Iron and Copper Nanoparticles in Aqueous Solution. *Chemosphere* **2023**, *324*, 138332. [CrossRef] [PubMed]
40. Chen, K.-Y.; Zeng, W.-Y. Adsorption of Cu(II) by Poly-γ-Glutamate/Apatite Nanoparticles. *Polymers* **2021**, *13*, 962. [CrossRef]
41. Tahir, H.; Anwer, M.; Khan, S.; Saad, M. Enhancement of Adsorption and Photocatalytic Activity of MgO Nanoparticles for the Treatment of Textile Dye Using Ultrasound Assisted Process by Response Surface Methodology. *Desalination Water Treat.* **2024**, *319*, 100429. [CrossRef]
42. Alam, S.; Ullah, R.; ur Rahman, N.; Ilyas, M.; Ullah, S.; Zahoor, M.; Umar, M.N.; Ullah, R.; Ali, E.A. Synthesis of Metallic Nanoparticles and Its Application in Adsorption of Metanil Yellow and Rhodamine B from Aqueous Solutions. *Desalination Water Treat.* **2023**, *313*, 186–195. [CrossRef]
43. Zhang, N.; Reguyal, F.; Sarmah, A.K. Effect of Iron Nanoparticles on Chromium Adsorption in Aqueous Solution Using Magnetic Biochar: A Site Energy Distribution Analysis. *Environ. Pollut.* **2024**, *346*, 123593. [CrossRef]
44. Cheperli, A.; Mokaber-Esfahani, M.; Taleghani, A.; Bahalkeh, F. Biosynthesis, Characterization and Antimicrobial Activities of Zinc Oxide Nanoparticles from Leaf and Seed Extracts of Malva Neglecta Wallr. *Inorg. Nano-Met. Chem.* **2024**. [CrossRef]
45. Elbrolesy, A.; Abdou, Y.; Elhussiny, F.A.; Morsy, R. Novel Green Synthesis of UV-Sunscreen ZnO Nanoparticles Using Solanum Lycopersicum Fruit Extract and Evaluation of Their Antibacterial and Anticancer Activity. *J. Inorg. Organomet. Polym. Mater.* **2023**, *33*, 3750–3759. [CrossRef]

46. Zhao, C.-Y.; Tan, S.-X.; Xiao, X.-Y.; Qiu, X.-S.; Pan, J.-Q.; Tang, Z.-X. Effects of Dietary Zinc Oxide Nanoparticles on Growth Performance and Antioxidative Status in Broilers. *Biol. Trace Elem. Res.* **2014**, *160*, 361–367. [CrossRef] [PubMed]
47. Brayner, R.; Ferrari-Iliou, R.; Brivois, N.; Djediat, S.; Benedetti, M.F.; Fiévet, F. Toxicological Impact Studies Based on Escherichia Coli Bacteria in Ultrafine ZnO Nanoparticles Colloidal Medium. *Nano Lett.* **2006**, *6*, 866–870. [CrossRef] [PubMed]
48. Sharifi-Rad, M.; Anil Kumar, N.V.; Zucca, P.; Varoni, E.M.; Dini, L.; Panzarini, E.; Rajkovic, J.; Tsouh Fokou, P.V.; Azzini, E.; Peluso, I.; et al. Lifestyle, Oxidative Stress, and Antioxidants: Back and Forth in the Pathophysiology of Chronic Diseases. *Front. Physiol.* **2020**, *11*, 694. [CrossRef] [PubMed]
49. Sies, H. Oxidative Stress: Concept and Some Practical Aspects. *Antioxidants* **2020**, *9*, 852. [CrossRef]
50. Pizzino, G.; Irrera, N.; Cucinotta, M.; Pallio, G.; Mannino, F.; Arcoraci, V.; Squadrito, F.; Altavilla, D.; Bitto, A. Oxidative Stress: Harms and Benefits for Human Health. *Oxid. Med. Cell. Longev.* **2017**, *2017*, 8416763. [CrossRef] [PubMed]
51. Ilyasov, I.R.; Beloborodov, V.L.; Selivanova, I.A.; Terekhov, R.P. ABTS/PP Decolorization Assay of Antioxidant Capacity Reaction Pathways. *Int. J. Mol. Sci.* **2020**, *21*, 1131. [CrossRef] [PubMed]
52. Munteanu, I.G.; Apetrei, C. Analytical Methods Used in Determining Antioxidant Activity: A Review. *Int. J. Mol. Sci.* **2021**, *22*, 3380. [CrossRef] [PubMed]
53. Payne, A.C.; Mazzer, A.; Clarkson, G.J.J.; Taylor, G. Antioxidant Assays—Consistent Findings from FRAP and ORAC Reveal a Negative Impact of Organic Cultivation on Antioxidant Potential in Spinach but Not Watercress or Rocket Leaves. *Food Sci. Nutr.* **2013**, *1*, 439–444. [CrossRef] [PubMed]
54. Donmez, S.; Keyvan, E. Green Synthesis of Zinc Oxide Nanoparticles Using Grape Seed Extract and Evaluation of Their Antibacterial and Antioxidant Activities. *Inorg. Nano-Met. Chem.* **2023**, *54*, 1137–1144. [CrossRef]
55. Tiwari, A.K.; Jha, S.; Tripathi, S.K.; Awasthi, R.R.; Bhardwaj, A.K.; Singh, A.K.; Dikshit, A. Antioxidant Response of *Calendula officinalis* L. Assisted Synthesized Zinc Oxide Nanoparticles. *Mater. Res. Express* **2024**, *11*, 085005. [CrossRef]

Disclaimer/Publisher's Note: The statements, opinions and data contained in all publications are solely those of the individual author(s) and contributor(s) and not of MDPI and/or the editor(s). MDPI and/or the editor(s) disclaim responsibility for any injury to people or property resulting from any ideas, methods, instructions or products referred to in the content.